Mem. S.A.It. Suppl. Vol. 19, 214

Memorie della
Supplementi

Galaxy metallicity near and far

F. Mannucci[1] and G. Cresci[1,2]

[1] Istituto Nazionale di Astrofisica – Osservatorio Astrofisico di Arcetri, Largo E. Fermi 5, I-50125, Firenze, Italy e-mail: filippo@arcetri.astro.it
[2] Max-Planck-Institut für extraterrestrische Physik (MPE), Giessenbachstr. 1, 85748, Garching, Germany

Abstract. Metallicity appears to be one the most important tool to study the formation and evolution of galaxies. Recently, we have shown that metallicity of local galaxies is tightly related not only to stellar mass, but also to star formation rate (SFR). At low stellar mass, metallicity decreases sharply with increasing SFR, while at high stellar mass, metallicity does not depend on SFR. The residual metallicity dispersion across this Fundamental Metallicity Relation (FMR) is very small, about 0.05 dex. High redshift galaxies, up to z∼2.5, are found to follow the same FMR defined by local SDSS galaxies, with no indication of evolution. At z>2.5, evolution of about 0.6 dex off the FMR is observed, with high-redshift galaxies showing lower metallicities. This result can be combined with our recent discover of metallicity gradients in three high redshift galaxies showing disk dynamics. In these galaxies, the regions with higher SFR also show lower metallicities. Both these evidences can be explained by the effect of smooth infall of gas into previously enriched galaxies, with the star-formation activity triggered by the infalling gas.

1. Introduction

Gas metallicity is regulated by a complex interplay between star formation, infall of metal-poor gas and outflow of enriched material. A fundamental discovery is the relation between stellar mass $M_\star$ and metallicity (McClure & van den Bergh 1968; Lequeux et al. 1979; Garnett 2002; Tremonti et al. 2004; Lee et al. 2006), with more massive galaxies showing higher metallicities. The origin of this relation is debated, and many different explanations have been proposed, including ejection of metal-enriched gas (e.g., Edmunds 1990; Lehnert & Heckman 1996; Tremonti et al. 2004), "downsizing", i.e., a systematic dependence of the efficiency of star formation on galaxy mass (e.g., Brooks et al. 2007; Mouchine et al. 2008; Calura et al. 2009), variation of the IMF with galaxy mass (Köppen et al. 2007), and infall of metal-poor gas (Finlator & Davé 2008; Davé et al. 2010).

The mass-metallicity relation has been studied by Erb et al. (2006) at z∼2.2 and by Maiolino et al. (2008) and Mannucci et al. (2009) at z=3–4, finding a strong and monotonic evolution, with metallicity decreasing with redshift at a given mass (see fig.1). The same authors (Erb et al. 2006; Erb 2008; Mannucci et al. 2009) have also studied the relation between metallicity and gas fraction, i.e., the effective yields, obtaining clear evidence of the importance of infall in high redshift galaxies.

If infall is at the origin of the star formation activity, and outflows are produced by exploding supernovae (SNe), a relation between

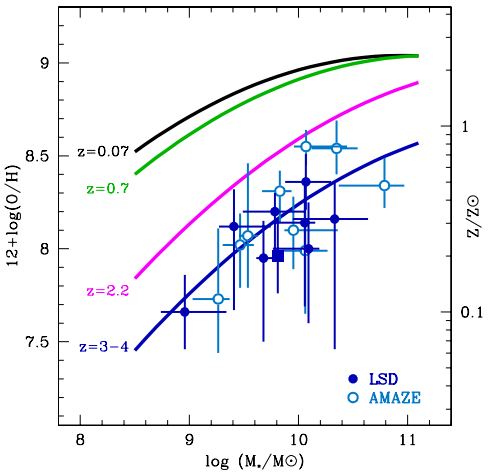

Fig. 1. Evolution of the mass-metallicity relation from local to high redshift galaxies from Mannucci et al. (2009). Data are from Kewley & Ellison (2008) (z=0.07), Savaglio et al. (2005) (z=0.7), Erb et al. (2006) (z=2.2) and Mannucci et al. (2009) (z=3–4).

metallicity and SFR is likely to exist. In other words, SFR is a parameter that should be considered in the scaling relations that include metallicity, such as the mass-metallicity relation.

2. The local Fundamental Metallicity Relation

To test the hypothesis of a correlation between SFR and metallicity in the present universe and at high redshift, we have studied several samples of galaxies at different redshifts whose metallicity, $M_\star$, and SFR have been measured. A full description of the data set is given in Mannucci et al. (2010).

Local galaxies are well measured by the SDSS project (Abazajian et al. 2009). Among the $\sim 10^6$ galaxies with observed spectra, we selected star forming objects with redshift between 0.07 and 0.30, having a signal-to-noise ratio (SNR) of Hα of SNR>25 and dust extinction $A_V < 2.5$. Total stellar masses $M_\star$ from Kauffmann et al. (2003) were used, scaled to the Chabrier (2003) initial mass function (IMF). SFRs inside the spectroscopic aperture were measured from the Hα emission line flux corrected for dust extinction as estimated from the Balmer decrement. The conversion factor between Hα luminosity and SFR in Kennicutt (1998) was used, corrected to a Chabrier (2003) IMF. Oxygen gas-phase abundances were measured from the emission line ratios as described in Maiolino et al. (2008). An average between the values obtain from [NII]λ6584/Hα and R23=([OII]λ3727+[OIII]λ4958,5007)/Hβ was used. The final galaxy sample contains 141825 galaxies.

The grey-shaded area in the left panel of Fig. 2 shows the mass-metallicity relation for our sample of SDSS galaxies. Despite the differences in the selection of the sample and in the measure of metallicity, our results are very similar to what has been found by Tremonti et al. (2004). The metallicity dispersion of our sample, ~0.08 dex, is somewhat smaller to what have been found by these authors, ~0.10 dex, possibly due to different sample selections and metallicity calibration.

The left panel of Fig. 2 also shows, as a function of $M_\star$, the median metallicities of SDSS galaxies having different levels of SFR. It is evident that a systematic segregation in SFR is present in the data. While galaxies with high $M_\star$ (log($M_\star$)>10.9) show no correlation between metallicity and SFR, at low $M_\star$ more active galaxies also show lower metallicity. The same systematic dependence of metallicity on SFR can be seen in the right panel of Fig. 2, where metallicity is plotted as a function of SFR for different values of mass. Galaxies with high SFRs show a sharp dependence of metallicity on SFR, while less active galaxies show a less pronounced dependence.

The dependence of metallicity on $M_\star$ and SFR can be better visualized in a 3D space with these three coordinates, as shown in Figure 3. SDSS galaxies appear to define a tight surface in the space, the Fundamental Metallicity Relation (FMR). The introduction of the FMR results in a significant reduction of residual metallicity scatter with respect to the simple mass-metallicity relation. The dispersion of individual SDSS galaxies around the FMR, is ~0.06 dex when computed across the full FMR and reduces to ~0.05 dex i.e, about 12%, in the

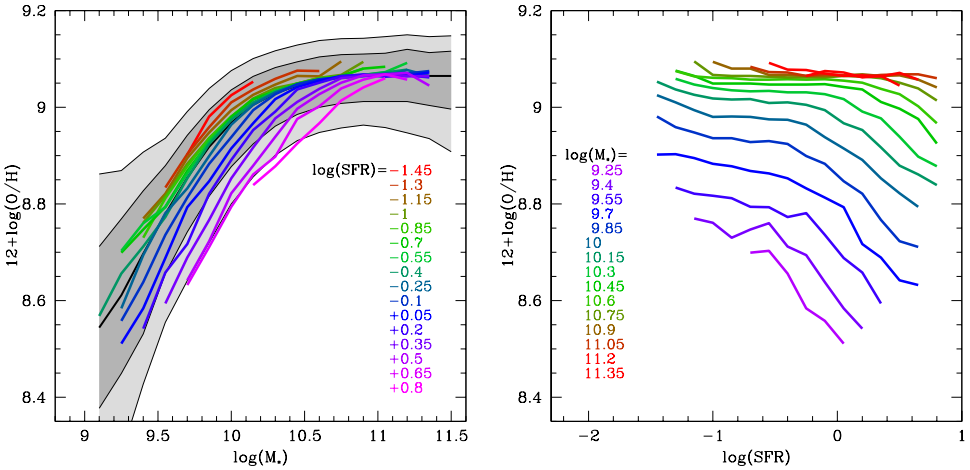

Fig. 2. *Left panel:* The mass-metallicity relation of local SDSS galaxies. The grey-shaded areas contain 64% and 90% of all SDSS galaxies, with the thick central line showing the median relation. The colored lines show the median metallicities, as a function of $M_\star$, of SDSS galaxies with different values of SFR. *Right panel:* median metallicity as a function of SFR for galaxies of different $M_\star$. At all $M_\star$ with log($M_\star$)<10.7, metallicity decreases with increasing SFR at constant mass .

central part of the relation where most of the galaxies are found. The final scatter is consistent with the intrinsic uncertainties in the measure of metallicity (~0.03 dex for the calibration, to be added to the uncertainties in the line ratios), on mass (estimated to be 0.09 dex by Tremonti et al. 2004), and on the SFR, which are dominated by the uncertainties on dust extinction.

The reduction in scatter with respect to the mass-metallicity relation becomes even more significant when considering that most of the galaxies in the sample cover a small range in SFR, with 64% of the galaxies ($\pm1\sigma$) is contained inside 0.8 dex. The mass-metallicity relation is not an adequate representation of galaxy samples with a larger spread of SFRs, as usually find at intermediate redshifts.

3. The FMR at high-redshift

The local galaxies can be compared with several samples of high-redshift objects. We extracted from the literature samples of galaxies in four redshift bins, for a total of ~300 objects, having published values of emission line fluxes, $M_\star$, and dust extinction: 0.5<z<0.9 (Savaglio et al. 2005, GDDS galaxies), 1.0<z<1.6 (Shapley et al. 2005; Liu et al. 2008; Wright et al. 2009; Epinat et al. 2009), 2.0<z<2.5 (Erb et al. 2006; Law et al. 2009; Lehnert et al. 2009; Förster Schreiber et al. 2009), and 3.0<z<3.7 (Maiolino et al. 2008; Mannucci et al. 2009). The same procedure used for the SDSS galaxies was applied to these galaxies.

Galaxies at all redshifts follow well defined mass-metallicity relations (see, for example, Mannucci et al. 2009, and references therein). For this reason each of these samples, except the one an z~3.3 that contains 16 objects only, is divided into two equally-numerous samples of low- and high-$M_\star$ objects. Median values of $M_\star$, SFR and metallicities are computed for each of these samples.

Galaxies up to z~2.5 follow the FMR defined locally, with no sign of evolution. This is an unexpected result, as simultaneously the mass-metallicity relation is observed to evolve rapidly with redshift (see Fig.1). The solution of this apparent paradox is that distant galaxies have, on average, larger SFRs, and, therefore, fall in a different part of the same FMR.

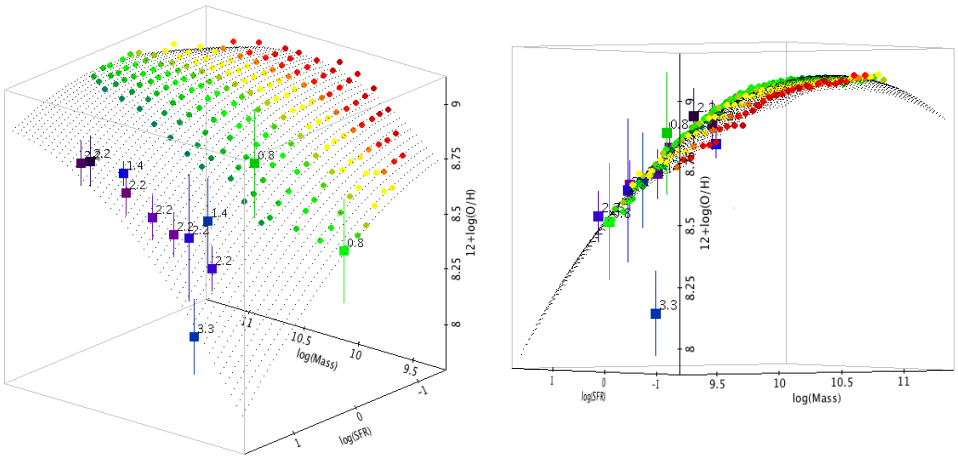

Fig. 3. Two projections of the Fundamental Metallicity Relation among $M_\star$, SFR and gas-phase metallicity. Circles without error bars are the median values of metallicity of local SDSS galaxies in bin of $M_\star$ and SFR, color-coded with SFR as shown in the colorbar on the right. These galaxies define a tight surface in the 3D space, with dispersion of single galaxies around this surface of ~0.05 dex. The black dots show a second-order fit to these SDSS data, extrapolated toward higher SFR. Square dots with error bars are the median values of high redshift galaxies, as explained in the text. Labels show the corresponding redshifts. The projection on the right emphasizes that most of the high-redshift data, except the point at z=3.3, are found on the same surface defined by low-redshift data.

In the SDSS sample, metallicity changes more with $M_\star$ (~0.5 dex from one extreme to the other at constant SFR, see Fig. 2) than with SFR (~0.30 dex at constant mass). Therefore mass is the main driver of the level of chemical enrichment of SDSS galaxies. This is related to the fact that galaxies with high SFRs, the objects showing the strongest dependence of metallicity on SFR (see the right panel of fig. 2), are quite rare in the local universe. At high redshifts, mainly active galaxies are selected, and the dependence of metallicity on SFR becomes dominant.

Galaxies at z~3.3 show metallicities lower of about 0.6 dex with respect to both the FMR defined by the SDSS sample and galaxies at 0.5<z<2.5. This is an indication that some evolution of the FMR appears at z>2.5, although its size can be affected several potential biases (see Mannucci et al. 2010 for a full discussion). A larger data set at z>3 is needed to solve this question.

4. What the FMR is telling us

The interpretation of these results must take into account several effects. In principle, metallicity is a simple quantity as it is dominated by three processes: star formation, infall, outflow. If the scaling laws of each of these three processes are known, the dependence of metallicity on SFR and $M_\star$ can be predicted. In practice, these three processes have a very complex dependence on the properties of the galaxies, and can introduce scaling relations in many different ways. First, it is not known how *outflows*, due to either SNe or AGNs, depend on the properties of the galaxies. Second, *infalls* of pristine gas are expected to influence metallicity in two ways: metallicity can be reduced by the direct accretion of metal-poor gas, and can be increased by the star formation activity which is likely to follow accretion. Third, the star formation activity is known to depend on galaxy mass, with heavier galaxies forming a larger fraction of stars at higher red-

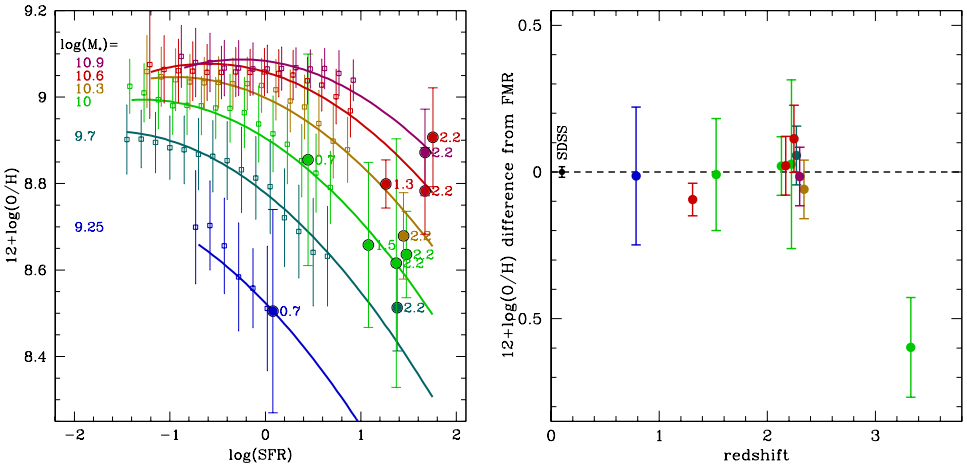

Fig. 4. *Left:* Metallicity as a function of SFR for galaxies in the three bins of $M_\star$ containing high-redshift galaxies. The values of log($M_\star$) are shown by the labels on the left. Empty square dots are the median values of metallicity of local SDSS galaxies, with error bars showing 1σ dispersions. Lines are the fits to these data. Solid dots are median values for high-redshift galaxies with z<2.5 in the same mass bins, with labels showing redshifts. *Right:* metallicity difference from the FMR for galaxies at different redshifts, color-coded in mass as in the left panel. The SDSS galaxies defining the relation are showing at z∼0.1 with their dispersion around the FMR. All the galaxy samples up to z=2.5 are consistent with no evolution of the FMR defined locally. Metallicities lower by ∼0.6 dex are observed at z∼3.3.

shifts, and this effect produce higher metallicities in more massive galaxies.

The dependence of metallicity on SFR can be explained by the dilution effect of the infalling gas. A simple model can be constructed (see Mannucci et al. 2010) where a variable amount of metal-poor, infalling gas, forming stars according to the Schmidt-Kennicutt law, can explain the dependence of metallicity on SFR. For this scenario to work, the timescales of chemical enrichment must be longer than the dynamical scales of the galaxies, over which the SFR is expected to evolve. In other words, galaxies on the FMR are in a *transient phase*: after an infall, galaxies first evolve towards higher SFR and lower metallicities. Later, while gas is converted into stars and new metals are produced, either galaxies drop out of the sample because they have faint Hα, or evolve toward higher values of mass and metallicities along the FMR. In this scenario, the dependence of metallicity on SFR is due to infall and dominates at high redshifts, where galaxies with massive infalls and large SFRs are found. In contrast, in the local universe such galaxies are rare, most of the galaxies have low level of accretion, and abundances are dominated by the dependence on mass, possibly due to outflow.

In many local galaxies, timescales of chemical enrichment can be shorter than the other relevant timescales (e.g., Silk 1993), and galaxies can be in a *quasi steady-state situation*, in which gas infall, star formation and metal ejection occur simultaneously (Bouché et al. 2010). Assuming this quasi steady-state situation, in which infall and SFR are slowly evolving with respect to the timescale of chemical enrichment, it can be shown (Mannucci et al. 2010) that our results support a scenario where outflows are inversely proportional to mass and increase with SFR$^{0.65}$.

The small scatter of SDSS galaxies around the FMR can be used to constrain the characteristics of gas accretion. For this infall/outflow scenario to work and produce a very small scat-

ter round the FMR, two conditions are simultaneously required: (1) star formation is always associated to the same level of metallicity dilution due to infall of metal-poor gas; (2) there is a relation between the amount of infalling and outflowing gas and the level of star formation. These conditions for the existence of the FMR fit into the smooth accretion models proposed by several groups (Bournaud & Elmegreen 2009; Dekel et al. 2009), where continuos infall of pristine gas is the main driver of the grow of galaxies. In this case, metal-poor gas is continuously accreted by galaxies and converted in stars, and a long-lasting equilibrium between gas accretion, star formation, and metal ejection is expected to established.

5. Abundance gradients in high-redshift galaxies

Recently (Cresci et al. 2010), we have obtained a direct evidence of the presence of smooth accretion of gas in high redshift galaxies. We selected three Lyman-break galaxies among the AMAZE (Maiolino et al. 2008) and LSD (Mannucci et al. 2009) samples which show a remarkably symmetric velocity field in the [OIII] emission line, which traces the ionized gas kinematics (see Fig. 4). Such kinematics indicates that these are rotationally supported disks (Gnerucci et al., in preparation), with no evidence for more complex merger-induced dynamics. Near-infrared spectroscopic observations of the galaxies were obtained with the integral field spectrometer SINFONI on VLT, and we used the flux ratios between the main rest-frame optical lines to obtain the metallicity map shown in Fig. 4. An unresolved region with lower metallicity is evident in each map, surrounded by a more uniform disk of higher metal content. In one case, CDFa-C9, the lower metallicity region is coincident with the galaxy center, as traced by the continuum peak, while it is offset by $\sim 0.60''$ (4.6 kpc) in SS22a-C16 and $\sim 0.45''$ (3.4 kpc) in SS22a-M38. On the other hand, in all the galaxies the area of lower metallicity is coincident or closer than $0.25''$ (1.9 kpc, half of the PSF FWHM) to the regions of enhanced line emission, tracing the more active star forming regions. The average difference between high and low metallicity regions in the three galaxies is 0.55 in units of 12+log(O/H), larger than the $\sim 0.2 - 0.4$ dex gradients measured in the Milky Way and other local spirals (van Zee et al. 1998) on the same spatial scales. The measured gas phase abundance variations have a significance between 98% and 99.8% . It can be shown (Cresci et al. 2010) that variations of ionization parameter across the galaxies cannot explain the observed gradients of line ratios, and that different metallicities are really requested.

Current models of chemical enrichment in galaxies (Molla et al. 1997) cannot reproduce our observations at the moment, as they assume radially isotropic gas accretion onto the disk and the instantaneous recycling approximation. Nevertheless, the detected gradients can be explained in the framework of the cold gas accretion scenario (Kereš et al. 2005) recently proposed to explain the properties of gas rich, rotationally supported galaxies observed at high redshift (Cresci et al. 2009; Förster Schreiber et al. 2009). In this scenario, the observed low metallicity regions are created by the local accretion of metal-poor gas in clumpy streams (Dekel et al. 2009), penetrating deep onto the galaxy following the potential well, and sustaining the observed high star formation rate in the pre-enriched disk. Stream-driven turbulence is then responsible for the fragmentation of the disks into giant clumps, as observed at $z \geq 2$ (Genzel et al. 2008; Mannucci et al. 2009), that are the sites of efficient star formation and possibly the progenitors of the central spheroid. This scenario is also in agreement with the dynamical properties of our sample, which appears to be dominated by gas rotation in a disk with no evidence of the dynamical asymmetries typically induced by mergers. The study of the relations between metallicity gas fractions, effective yields, and SFR (Cresci et al. 2010) shows that the low-metallicity regions can be well explained by amounts of infalling gas much larger than in the remaining high-metallicity regions.

Our observations of low metallicity regions in these three galaxies at $z \sim 3$ therefore provide the evidence for the actual presence of

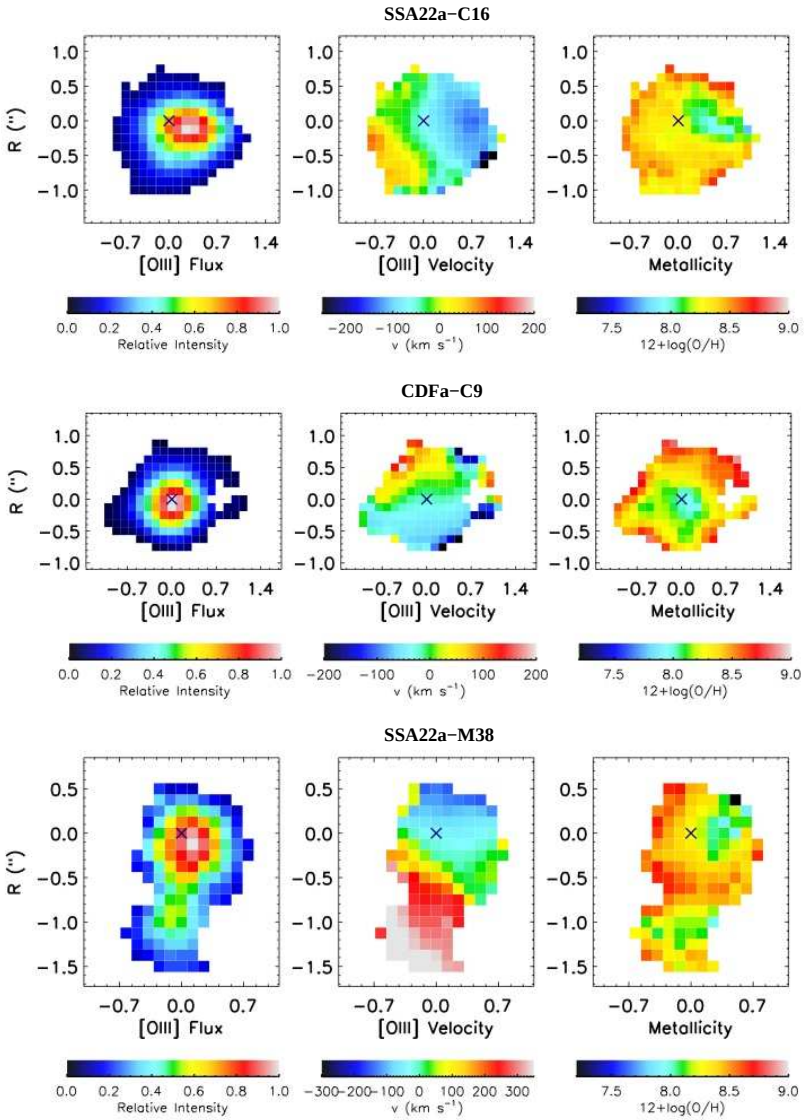

Fig. 5. Surface brightness of the [OIII]λ5007 line, velocity map, and gas phase metallicity, plotted as relative abundances of oxygen and hydrogen parameterized in units of $12 + log(O/H)$, of the three galaxies in Cresci et al. (2010). Lower metallicity region are surrounded by a more enriched disk. The crosses in each panel mark the position of the continuum peak.

accretion of metal-poor gas in massive high-z galaxies, capable to sustain high star formation rates without frequent mergers of already evolved and enriched sub-units. This picture was already indirectly suggested by recent observational studies of gas rich disks at $z \sim 1-2$ (Förster Schreiber et al. 2009; Tacconi et al. 2010), and is in agreement with the FMR described above.

References

Abazajian, et al. 2009, ApJS, 182, 543

Bouché, et al. 2010, ApJ, 718, 1001
Bournaud, F. & Elmegreen, B. G. 2009, ApJL, 694, L158
Brooks, A. M., et al. 2007, ApJL, 655, L17
Calura, F., et al. 2009, A&A, 504, 373
Chabrier, G. 2003, PASP, 115, 763
Cresci, G., et al. 2009, ApJ, 697, 115
Cresci, G., et al. 2010, Nature, 467, 811
Davé, et al. 2010, MNRAS, 404, 1355
Dekel, A., Sari, R., & Ceverino, D. 2009, ApJ, 703, 785
Edmunds, M. G. 1990, MNRAS, 246, 678
Epinat, B., et al. 2009, A&A, 504, 789
Erb, D. K. 2008, ApJ, 674, 151
Erb, D. K., et al. 2006, ApJ, 644, 813
Finlator, K. & Davé, R. 2008, MNRAS, 385, 2181
Förster Schreiber, et al. 2009, ApJ, 706, 1364
Garnett, D. R. 2002, ApJ, 581, 1019
Genzel, R., et al. 2008, ApJ, 687, 59
Kauffmann, et al. 2003, MNRAS, 341, 33
Kennicutt, Jr., R. C. 1998, ARAA, 36, 189
Kereš, D., Katz, N., Weinberg, D. H., & Davé, R. 2005, MNRAS, 363, 2
Kewley, L. J. & Ellison, S. L. 2008, ApJ, 681, 1183
Köppen, J., Weidner, C., & Kroupa, P. 2007, MNRAS, 375, 673
Law, D. R., et al. 2009, ApJ, 697, 2057
Lee, H., et al. 2006, ApJ, 647, 970
Lehnert, M. D. & Heckman, T. M. 1996, ApJ, 462, 651
Lehnert, M. D., et al. 2009, ApJ, 699, 1660
Lequeux, J., et al. 1979, A&A, 80, 155
Liu, X., et al. 2008, ApJ, 678, 758
Maiolino, R., et al. 2008, A&A, 488, 463
Mannucci, F., et al. 2010, MNRAS, 408, 2115
Mannucci, F., et al. 2009, MNRAS, 398, 1915
McClure, R. D. & van den Bergh, S. 1968, AJ, 73, 1008
Molla, M., Ferrini, F., & Diaz, A. I. 1997, ApJ, 475, 519
Mouchine, M., Gibson, B. K., Renda, A., & Kawata, D. 2008, ArXiv e-prints
Savaglio, S., et al. 2005, ApJ, 635, 260
Shapley, A. E., Coil, A. L., Ma, C.-P., & Bundy, K. 2005, ApJ, 635, 1006
Silk, J. 1993, Proceedings of the National Academy of Science, 90, 4835
Tacconi, L. J., et al. 2010, Nature, 463, 781
Tremonti, C. A., et al. 2004, ApJ, 613, 898
van Zee, L., et al. 1998, AJ, 116, 2805
Wright, S. A., et al. 2009, ApJ, 699, 421